

Shape control of cable structures considering concurrent/sequence control

Sudeok Shon^{1a}, Alan S. Kwan^{2b} and Seungjae Lee^{*1}

¹*School of Architectural Engineering, Korea University of Technology and Education, Cheonan, Chungnam 330-708, Republic of Korea*

²*Cardiff School of Engineering, Cardiff University, Parade, Cardiff CF24-3AA, UK*

(Received March 5, 2013, Revised May 10, 2014, Accepted June 9, 2014)

Abstract. In this study, the control of the shape of pre-stressed cable structures and the effective control element were examined. The process of deriving the displacement control equations using the force method was explained, and the concurrent control scheme (CCS) and the sequence control scheme (SCS) were proposed. To explain the control scheme process, the quadrilateral cable net model was adopted and classified into a regular model and an irregular model for the analysis of the control results. In the control analysis of the regular model, the CCS and SCS analysis results proved reliable. For the SCS, the errors occur in the control stage and varied according to the control sequence. In the control analysis of the irregular model, the CCS analysis result also proved relatively reliable, and the SCS analysis result with the correction of errors in each stage was found nearly consistent with the target shape after the control. Finally, to investigate an effective control element, the Geiger cable dome was adopted. A set of non-redundant elements was evaluated in the reduced row echelon form of a coefficient matrix of control equations. Important elements for shape control were also evaluated using overlapping elements in the element sets, which were selected based on cable adjustments.

Keywords: shape adjustment; pre-stressed cable structures; force method; concurrent control; sequence control; non-redundant element; reduced row echelon form

1. Introduction

The field of shape control, a branch of control engineering, plays a crucial role in the correction and adjustment of the shapes of space antennae and other structures that require precise shapes, of smart structures that can adjust and respond to diverse internal and external conditions, and of cable nets and other flexible structures. Shapes such as those of pin-joint assemblers, which are defined by the joint locations, undergo a very precise manufacturing process; but due to their initial imperfections, that is, errors in their manufacture, thermal expansion, unexpected load or pre-stressing, unplanned shapes may be formed. Notably, when the shape of a cable structure is

*Corresponding author, Professor, E-mail: leeseung@koreatech.ac.kr

^aProfessor, E-mail: sdshon@koreatech.ac.kr

^bPh.D., E-mail: kwan@cardiff.ac.uk

deformed due to the loosening tension of the structure, it is very important to correct it to maintain the structural completeness or to maintain/repair the structure.

Initial stage researches on the shape control of large space antennae and other large-scale structures were conducted by Haftka *et al.* (1985a, b). They studied the analytical process of element adjustment in the quasi-steady-state deformation of the original shape under temperatures, and on the location of actuators, using experimental approach. Quoting from this paper, Irschik (2002) defined the objective of shape control as the use of an adjustment device and the removal of the impact of certain external disturbances on the deformation of a structure. Furthermore, Burdisso and Haftka (1990) studied an effective analysis method for quasi-static shape control, and Furuya and Haftka (1995a, b), using genetic algorithms, studied the optimal location of the element control device considering the number of control sensors and actuators. Subramanian and Mohan (1996) examined these indirect approaches with their successive peak error algorithms using heuristic method, and Shea *et al.* (2002) published a paper on the development of intelligent tensegrity structures using a stochastic search method.

To maintain the originally designed shape of frame structures, Irschik *et al.* (1998) proposed a direct analysis solution designed to evaluate the eigenstrain distribution to incapacitate or minimize the expected load, and attempted to apply the concept of stress-free eigenstrain in generalizing the problem of the static shape control of objects that create strain due to external force (Irschik and Ziegler 2001). Regarding various approaches, Ziegler (2005) studied a method of directly evaluating a quasi-static shape control solution, applied the method to thin revolution shells, discontinuous structures, etc., and thus, expanded its applications. Nyashin *et al.* (2005) studied shape control by evaluating an explicit relational expression between nodal displacement and impotent eigenstrain. In addition, some shape control methods of deployable cable net reflectors have been investigated. (Tanaka and Natori 2006, Tanaka *et al.* 2008, Tanaka 2011), and also some studies for shape control of cable net structures have recently been investigated.

On the other hand, You (1997) studied a direct method of controlling the displacement of truss/cable structures while retaining the minimum pre-stressing level; and based on the force method, derived the relationship between the element's elongation and the displacement. Before this, in the paper of Kwan *et al.* (1993), although they did not purport to control shapes or displacement, they proposed a more general method of calculating the actuator location and the length adjustment to create an internal force pattern that is necessary in the pre-stress state. Kim *et al.* (2003), Jeong *et al.* (2004) studied and analyzed the shape control of cable domes using the finite element method, which, however, was not more intuitive than the force method in terms of the initial tension for the shape control. Various stages of the control process had the shortcomings of their control element selection having to undergo trials and errors. Unlike the control using the finite element method, the control method of Kwan *et al.* (1993), You (1997), which is based on the force method, although not considering the control sequence, is a direct method of directly obtaining the elongation of the element.

A cable structure is relatively light and is designed using the minimal surface theory, which makes it optimal to plan a spatial structure. In this cable structures, the shape of cable net depends on the pre-stress distribution in cables, and the pre-stresses are inter-coupled. (Li and Wang 2009, Li and Ma 2011, Liu *et al.* 2012) Because of its advantages of low mass, high stiffness, and extension, cable structures have recently gained wide acceptance in the fields of architectures and space structures. (Zribi *et al.* 2006, Quelle 2009) However, it is difficult to construct a cable structure that is shaped as intended by the designer, and to continue to retain the initial shape; and much research on the control sequence and methods is needed. This paper dwelt on the adjustment

of shapes that are strained in pre-stressed cable structures due to tension loosening. The concurrent control scheme (CCS) and the sequence control scheme (SCS) using the force method were proposed, quadrilateral cable net structures were used and applied, and the resulting reliability was investigated. The method of evaluating the effective control element was also proposed using cable dome models. This paper has the following composition. Chapter 2 explains the process of deriving the shape control equations, and Chapter 3 discusses the CCS and the SCS using the control equations. Also, targeting the quadrilateral cable net model, which is classified into regular and irregular models, the analysis results and reliability of the control schemes are compared. Chapter 4, for the selection of the effective control element, proposes a method of evaluating the important elements according to the reduced row echelon form (RREF) and the control amount, targeting Geiger cable dome. Finally, Chapter 5 summarizes the findings of this study.

2. Control equations using the force method

Unlike the displacement method, the force method has a less complicated relationship between the displacement vector and the internal force vector, which makes it more accessible and enables intuitive understanding of structures. When the external load vector is set as \mathbf{p} , and the element's internal force vector, as \mathbf{t} , the equilibrium equations of structures can be formulated as shown in Eq. (1), which calculates the equilibrium of the external load and the internal force.

$$\mathbf{A}\mathbf{t} = \mathbf{p} \quad (1)$$

The compatibility of the displacement vector \mathbf{d} with the element's elongation vector \mathbf{e} is shown in Eq. (2). Here, matrix \mathbf{B} is the transpose matrix of \mathbf{A} , and the two matrixes provide various information for the assessment of the status of the structure (Pellegrino 1993).

$$\mathbf{B}\mathbf{d} = \mathbf{e} \quad (2)$$

As for the third relational expression, the structure that satisfies equilibrium and compatibility should also has the relationship as shown in Eq. (3) between the internal force and strain, in which matrix \mathbf{F} is a flexibility matrix.

$$\mathbf{F}\mathbf{t} = \mathbf{e} \quad (3)$$

General solutions to the equilibrium equations consist of particular solutions to the non-homogeneous equations and of general solutions of the homogeneous equations. Thus, one of the solutions to the non-homogeneous equations is Eq. (4), and \mathbf{A}^+ is a pseudo-inverse of \mathbf{A} .

$$\mathbf{t}_A = \mathbf{A}^+\mathbf{p} \quad (4)$$

Here, if nullspace of \mathbf{A} is \mathbf{S} , the general solution to the homogeneous equations consists of the combination coefficient $\boldsymbol{\alpha}$, and thus, Eq. (5) can be a general solution to the equilibrium equations.

$$\mathbf{t} = \mathbf{t}_A + \mathbf{S}\boldsymbol{\alpha} \quad (5)$$

If the initial strain is defined as \mathbf{e}_0 and Eq. (5) is substituted into Eq. (3), the following relational expression can be evaluated. Here, by finding $\boldsymbol{\alpha}$, the structure can be analyzed.

$$\mathbf{e} = \mathbf{e}_0 + \mathbf{F}\mathbf{t} = \mathbf{e}_0 + \mathbf{F}\{\mathbf{t}_A + \mathbf{S}\boldsymbol{\alpha}\} \quad (6)$$

If matrix \mathbf{A} is identical to the transpose of matrix \mathbf{B} , matrix \mathbf{S} , which represents self-equilibrium, is actually identical with the nullspace (\mathbf{A}) and the elongation vector \mathbf{e} must be orthogonal to the left-nullspace (\mathbf{B}). Thus, compatibility can be defined by Eq. (7).

$$\mathbf{S}^T \mathbf{e} = \mathbf{0} \quad (7)$$

If Eq. (6) is substituted into the Eq. (7), $\boldsymbol{\alpha}$ can be expressed by Eq. (8); and if Eq. (8) is substituted into Eq. (5), the internal force of the structure can be calculated.

$$\boldsymbol{\alpha} = -(\mathbf{S}^T \mathbf{F} \mathbf{S})^{-1} [\mathbf{S}^T \mathbf{e}_0 + \mathbf{S}^T \mathbf{F} \mathbf{t}_A] \quad (8)$$

Here, Eq. (8) consists of the sum of terms \mathbf{e}_0 and \mathbf{t}_A , with the first term referring to the effect on the initial strain, and the second term, to the displacement created due to the external load.

If Eq. (6) and (8) are substituted into the Eq. (2) to establish an equations for displacement control, and if the result is arranged according to term \mathbf{e}_0 , Eq. (9) can be obtained. Term \mathbf{e}_0 can be divided into the control vector \mathbf{e}_{adj} and the initial strain \mathbf{e}_{ini} .

$$\mathbf{d} = \mathbf{B}^+ \mathbf{e} = \mathbf{Y} \mathbf{e}_0 + \mathbf{d}_p = \mathbf{Y} \{ \mathbf{e}_{ini} + \mathbf{e}_{adj} \} + \mathbf{d}_p \quad (9)$$

The displacement in Eq. (9) has two terms. The first term is concerned with the initial strain and the second term \mathbf{d}_p is concerned with the external load \mathbf{p} of the structures. Thus, the vector \mathbf{d} is the displacement for the shape control, and the solution of the equations can be obtained by using the pseudo-inverse as follows

$$\mathbf{e}_{adj} = \mathbf{Y}^+ \{ \mathbf{d}_{ctrl} - \mathbf{Y} \mathbf{e}_{ini} - \mathbf{d}_p \} \quad (10)$$

A cable structure can be stabilized by introducing initial tension to it, and the corresponding deformed shape of the structure can be adjusted by evaluating the control vector in the Eq. (10). At this time, in the case of equilibrium-state of the structures with the initial tension, term \mathbf{d}_p is $\mathbf{0}$. As seen in the Eq. (10), the element control elongation \mathbf{e}_{adj} can be obtained using the element control equation as Eq. (10).

3. Shape control considering the control sequence

The shape of space antennae, trusses and other pin-joint assemblers as cable structures is usually defined by its nodal positions and controlling the shape requires control of the displacement of the nodes. If the derived displacement control equation as Eq. (10) is used, the element's control elongation \mathbf{e}_{adj} for maintaining the desired shape can be calculated directly. In this case, the control sequence of the elements is not considered; and if it is considered, the size of the errors will differ depending on the initial condition of the structure.

Thus, control procedures can be two different schemes. One is concurrent control (i.e., CCS), the other is sequence control in consideration of the order of the control member. Since both the CCS and the SCS can reach equilibrium after each control, the errors can be calculated through equilibrium analysis of the current state. In the case of the CCS using Eq. (10), the virtual codes are outlined as follows.

The structure, after the CCS control, reaches a new equilibrium, and \mathbf{e}_{adj} becomes equivalent to the initial strain \mathbf{e}_{ini} in the equilibrium analysis. Thus, according to the sequence, the SCS repeats as many equilibrium analyses as the number of controls using the CCS control and the control results. Here, the equilibrium analysis needs an analysis method that considers the initial

```

Start
Read Initial Data
Clear memory
Assemble matrix  $A$ ,  $B$ ,  $F$ ,  $p$ ,  $e_{ini}$  and  $d_{ctrl}$ 
  Calculate matrix  $S$  by using SVD algorithm
  Calculate vector  $t_A = A^+p$ 
  Calculate parameters  $\alpha$ 
  Calculate vector  $d_p$ 
  Calculate matrix  $Y$ 
Re-assemble  $Y$  by control elements
Decision of order of sequence control (by using RREF( $Y$ ) or  $\text{abs}(e_{adj})$ )
Solve  $e_{adj} = Y^+\{d_{ctrl} - Ye_{ini} - d_p\}$ 
Write results
Stop
End

```

Fig. 1 Virtual code of CCS (Concurrent Control Scheme)

```

Start
Read Initial Data
Clear memory
To do CCT analysis (see Fig.1) for decision of important element
Decision of order of sequence control (by using RREF( $Y$ ) or  $\text{abs}(e_{adj})$ )
Do loop n=1, total step of sequence control
  To do CCT analysis (see Fig.1) for current step
  (Calculate  $e_{adj}^{correct}$  for next step)
  Reassemble  $e_{ini}$ 
  To do Equilibrium analysis by using Gauss-Newton method (Kwan 1998)
  Write results
End Do
Stop
End

```

Fig. 2 Virtual code of SCS (Sequence Control Scheme)

Table 1 Coordinate of quadrilateral cable net (unit: cm)

| Node | 1 | 2 | 3 | 4 | 5 | 6 | 7 | 8 |
|------|--------|--------|-------|-------|--------|--------|-------|-------|
| X | -200.0 | 0.0 | 200.0 | 0.0 | -100.0 | 0.0 | 100.0 | 0.0 |
| Y | 0.0 | -200.0 | 0.0 | 200.0 | 0.0 | -100.0 | 0.0 | 100.0 |

stress and strain, and this study used the Kwan (1998) method that employs the Gauss-Newton (GN) method. To determine the control sequence, in the initial CCS analysis, the SCS may use the order of e_{adj} or the matrix Y 's RREF. Errors associated with the control sequence can be considered depending on the initial condition of the structure. Such a SCS control process can be expressed in Fig. 2 in terms of virtual codes.

To explain the shape control process, the quadrilateral cable net model shown in Fig. 3 is used. It has eight elements and eight nodes. Nodes 1-4 are fixed, and their nodal coordinates are shown in Table 1. This model was introduced by Kim *et al.* (2003), and the displaced nodes were

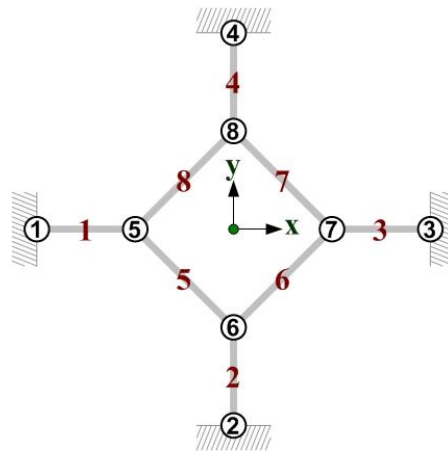


Fig. 3 Number of cables and nodes of quadrilateral cable net

Table 2 Information and target displacement of RCN model

| Case | Control elements | Material property | | Dir. | Target displacement (cm) (d_{tget}) | | | |
|------|------------------|-------------------|----------------------|------|---|--------|--------|--------|
| | | E (MPa) | A (cm ²) | | Node 5 | Node 6 | Node 7 | Node 8 |
| A | 1, 2, 3, 4 | 100.0 | 1.0 | X | -1.0 | 0.0 | 1.0 | 0.0 |
| | | | | Y | 0.0 | -1.0 | 0.0 | 1.0 |
| B | 1, 2, 3, 4 | 100.0 | 1.0 | X | -10.0 | 0.0 | 10.0 | 0.0 |
| | | | | Y | 0.0 | -10.0 | 0.0 | 10.0 |
| C | 5, 6, 7, 8 | 100.0 | 1.0 | X | -10.0 | 0.0 | 10.0 | 0.0 |
| | | | | Y | 0.0 | -10.0 | 0.0 | 10.0 |

controlled target positions using the initial tension. The adopted model, as introduced in literature, was handled by dividing it into a regular cable net (RCN) and an irregular cable net (IRCN). The former model is a virtual model that maintains the original shape and controls the nodes, and the latter model is a virtual model that restores the imperfect shape into the initial design shape.

3.1 RCN model

The RCN model is a virtual model designed to move free nodes as much to the outer direction as the target in the shape in Fig. 3. The target shape is shown in Fig. 4. The cable's elastic modulus E and the sectional area A are 100 MPa and 1.0 cm², respectively. The initial tension needed to maintain equilibrium state was 10 kN for elements 1-4, and 7.071 kN for elements 5-8. For the target model control, three cases, as shown in Table 2, were considered. First, Case A controlled the target displacement by as much as 1.0 cm to the exterior, and cases B and C moved it by as much as 10 cm. The control element controlled only the exterior cable (elements 1-4) in cases A and B, and Case C controlled the ring cable (elements 5-8).

Table 3 shows the results of the analysis of the RCN model using the CCS. The table contains the control amount e_{adj} according to the analysis results and the equilibrium results using the GN method. All the case results were consistent with the target displacement; and because the target shape was very simple, it was simply verified. Here, the displacement results in cases A and

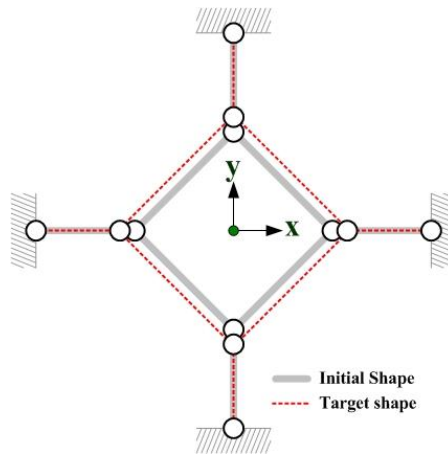


Fig. 4 Initial shape and target shape of RCN model

Table 3 Result of the analysis of the RCN model using the CCS method

| Case | Control elements | Initial Tension (kN) | e_{adj} (cm) | Result of GN method | | | | | |
|------|------------------|----------------------|----------------|---------------------|-----------|-------------------|-------|------|------|
| | | | | Tension (kN) | node Dir. | Displacement (cm) | | | |
| | | | | | | 5 | 6 | 7 | 8 |
| A | 1 2 3 4 | 10.0 | -2.4142 | 10.141 | X | -1.0 | 0.0 | 1.0 | 0.0 |
| | 5 6 7 8 | 7.071 | N.A. | 7.1711 | Y | 0.0 | -1.0 | 0.0 | 1.0 |
| B | 1 2 3 4 | 10.0 | -24.1421 | 11.414 | X | -10.0 | 0.0 | 10.0 | 0.0 |
| | 5 6 7 8 | 7.071 | N.A. | 8.071 | Y | 0.0 | -10.0 | 0.0 | 10.0 |
| C | 1 2 3 4 | 10.0 | N.A. | 8.999 | X | -10.0 | 0.0 | 10.0 | 0.0 |
| | 5 6 7 8 | 7.071 | -24.1421 | 6.363 | Y | 0.0 | -10.0 | 0.0 | 10.0 |

B were linearly related, which is a natural result of the characteristics of the target model. In cases B and C, the cable tension differed, but this work did not consider the cable tension

The RCN model control was analyzed using the SCS algorithms, and the analysis results for each case are shown in Table 4. Here, the control element was controlled in ascending order; and in the control stage, the error correction $e_{adj}^{correct}$ was not considered. As for Case A, the target displacement of which was one-tenth that of the other cases, the results of the SCS, although it did not consider the control-stage correction, were almost consistent with the target displacement d_{tget} . The maximum error of the analysis result was 0.004 cm. This figure is very minimal, given that the maximum length of the model was 400 cm. As for Case B, the target displacement alone of which was 10 times larger under the same condition, its error was larger than that of Case A compared to the CCS results. Its maximum error was 0.421cm, which is minimal compared to the model size but bigger than that of Case A. The linear relationship between the CCS analysis results for the two cases was not found in the SCS and slightly differed. The results for Case C with a different control element order produced an error similar to that of the results for Case B, which were bigger than those for Case A. In the case of the RCN model, if the target displacement to be controlled is small, the error produced in the control stage will be small.

In the case of the RCN model, the CCS method, given the results of the equilibrium analysis, made it possible to obtain a very accurate control result, and the SCS control, when the target

Table 4 Displacement results of the RCN model using the SCS method

| Node | | Case A | | | Case B | | | Case C | |
|------|---|------------|-----------|--------|------------|-----------|--------|-----------|--------|
| | | d_{tget} | d_{adj} | Error* | d_{tget} | d_{adj} | Error* | d_{adj} | Error* |
| 5 | X | -1.0 | -1.004 | 0.004 | -10.0 | -10.421 | 0.421 | -9.867 | -0.132 |
| | Y | 0.0 | -0.001 | 0.001 | 0.0 | -0.087 | 0.087 | 0.045 | -0.045 |
| 6 | X | 0.0 | -0.001 | 0.001 | 0.0 | -0.102 | 0.102 | 0.002 | -0.002 |
| | Y | -1.0 | -1.003 | 0.003 | -10.0 | -10.331 | 0.331 | -9.912 | -0.087 |
| 7 | X | 1.0 | 1.001 | -0.001 | 10.0 | 10.003 | -0.003 | 9.859 | 0.140 |
| | Y | 0.0 | -0.001 | 0.001 | 0.0 | -0.087 | 0.087 | 0.049 | -0.049 |
| 8 | X | 0.0 | -0.001 | 0.001 | 0.0 | -0.103 | 0.103 | 0.006 | -0.006 |
| | Y | 1.0 | 0.999 | 0.001 | 10.0 | 9.977 | 0.022 | 9.815 | 0.184 |

*Error = Target displacement (d_{tget}) – Control displacement (d_{adj})

Table 5 Coordinate and initial tension of the IRCN model (unit: cm and kN, respectively)

| Node | 1 | 2 | 3 | 4 | 5 | 6 | 7 | 8 |
|-----------------|--------|--------|-------|-------|---------|---------|--------|--------|
| X | -200.0 | 0.0 | 200.0 | 0.0 | -78.073 | 7.8214 | 104.46 | 7.1953 |
| Y | 0.0 | -200.0 | 0.0 | 200.0 | 4.341 | -89.604 | 3.7161 | 103.08 |
| Element | 1 | 2 | 3 | 4 | 5 | 6 | 7 | 8 |
| Initial Tension | 8.20 | 9.05 | 9.56 | 9.72 | 6.05 | 6.57 | 6.90 | 6.29 |

Table 6 Information and target displacement of the IRCN model

| Control elements | Material property | | Node Dir. | Target displacement (cm) d_{tget} | | | |
|------------------|-------------------|---------------------|-----------|-------------------------------------|---------|---------|---------|
| | E | A | | 5 | 6 | 7 | 8 |
| All | 10 GPa | 1.0 cm ² | X | -21.927 | -7.8214 | -4.46 | -7.1953 |
| | | | Y | -4.341 | -10.396 | -3.7161 | -3.08 |

displacement was small, did not need to consider the errors in the control process. In the case of a big target displacement, the error in the control process varied according to the selected control element, which is deemed to have been due to the geometric non-linearity in accordance with the control sequence.

3.2 IRCN model

If the initial shape in Fig. 3 is deformed into the shape in Fig. 5 due to the loosening of the cable tension, the IRCN model restores the deformed shape to the initially designed shape. The initial tension to be equilibrium with the nodal coordinate of the deformed shape in the figure is shown in Table 5. The cable's elastic modulus E and sectional area A were 10 GPa and 1.0 cm², respectively. The target displacement needed to restore the original shape is shown in Table 6, and the maximum target displacement was 21.927 cm. To restore the shape, the control elongation e_{adj} was calculated using the CCS method and the SCS method, and the results were compared.

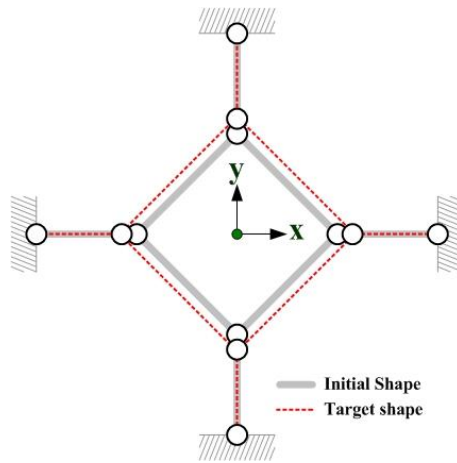


Fig. 5 Initial shape and target shape of the IRCN model

Table 7 Analysis result of the IRCN model based on the CCS method

| No. Element | Order | e_{adj} (cm) | Result of GN method | | | | | |
|-------------|-------|----------------|---------------------|-------------|----------------|-----------|------------|----------|
| | | | No. node | Coord. (cm) | d_{adj} (cm) | ERR* (%) | ERR0** (%) | |
| 1 | 1 | -22.06757 | 5 | X | -99.76919 | -21.69619 | 1.05265 | -0.05770 |
| 2 | 2 | -10.92276 | | Y | 0.19464 | -4.14636 | 4.48381 | -0.04866 |
| 3 | 7 | 4.31220 | 6 | X | 0.01933 | -7.80207 | 0.24717 | -0.00483 |
| 4 | 6 | 2.53884 | | Y | -100.07638 | -10.47238 | -0.73472 | 0.01910 |
| 5 | 3 | 13.98686 | 7 | X | 99.97565 | -4.48435 | -0.54601 | 0.00609 |
| 6 | 5 | 7.05820 | | Y | 0.11239 | -3.60371 | 3.02449 | -0.02810 |
| 7 | 8 | 2.36796 | 8 | X | -0.06216 | -7.25746 | -0.86386 | 0.01554 |
| 8 | 4 | 10.58291 | | Y | 100.18375 | -2.89625 | 5.96578 | -0.04594 |

$$*ERR=100 \times \frac{d_{tget}-d_{ctrl}}{d_{tget}} (\%), **ERR0=100 \times \frac{d_{tget}-d_{ctrl}}{\text{Maximum length of structures}} (\%)$$

The results of the CCS analysis of the IRCN model are shown in Table 7, and the maximum e_{adj} was 22.06757 cm. Given the results of the equilibrium analysis, the controlled displacement error (ERR) ranged from 0.24% to 5.97% compared with the target displacement, and the shape was almost consistent with the target shape. Given the maximum length 400 cm of the model, the error (ERR0) was 0.0048%-0.058%, which makes the analysis results reliable.

For the SCS analysis of the IRCN model, the control sequence was determined according to the control amount shown in Table 7; and as shown in Table 8, the elements were controlled in the following order: 1 → 2 → 5 → 8 → 7 → 6 → 4 → 3. The errors that were produced in the control process were corrected, and the corrected control amount $e_{adj}^{correct}$ slightly differed from that of the CCS analysis results. The maximum e_{adj} was 27.59547 cm, which was greater than that of the CCS results. Given the results of the equilibrium analysis, the ERR ranged from 0.001% to 0.066% compared with the target displacement, and the shape was almost consistent with the target shape. The error ERR0 ranged from 0.00005% to 0.0006%, which makes the result reliable.

Table 8 Results of the analysis of the IRCN model using the SCS method*

| No. Element | Order | $e_{adj}^{correct}$ (cm) | Result of GN method | | | | | |
|-------------|-------|--------------------------|---------------------|-------------|----------------|-----------|----------|---------|
| | | | No. node | Coord. (cm) | d_{adj} (cm) | ERR (%) | ERR0 (%) | |
| 1 | 1 | -27.59547 | 5 | X | -100.00025 | -21.92725 | -0.00114 | 0.00006 |
| 2 | 2 | -16.03444 | | Y | -0.00242 | -4.34342 | -0.05577 | 0.00061 |
| 3 | 8 | -0.02931 | 6 | X | -0.00063 | -7.82203 | -0.00799 | 0.00016 |
| 4 | 7 | -1.65695 | | Y | -100.00081 | -10.39681 | -0.00782 | 0.00020 |
| 5 | 3 | 9.98269 | 7 | X | 99.99981 | -4.46019 | -0.00428 | 0.00005 |
| 6 | 5 | 2.67252 | | Y | -0.00242 | -3.71852 | -0.06515 | 0.00061 |
| 7 | 6 | -2.14746 | 8 | X | -0.00063 | -7.19593 | -0.00870 | 0.00016 |
| 8 | 4 | 6.67183 | | Y | 99.99913 | -3.08087 | -0.02834 | 0.00022 |

*Sequence of SCS control: 1→2→5→8→7→6→4→3

Table 9 Results of the analysis of the IRCN model using the SCS method (double element Control)*

| No. Element | Order | $e_{adj}^{correct}$ (cm) | Result of GN method | | | | | |
|-------------|-------|--------------------------|---------------------|-------------|----------------|-----------|----------|----------|
| | | | No. node | Coord. (cm) | d_{adj} (cm) | ERR (%) | ERR0 (%) | |
| 1 | 1 | -25.53423 | 5 | X | -99.99982 | -21.92682 | 0.00083 | -0.00005 |
| 2 | 2 | -14.01978 | | Y | -0.00363 | -4.34463 | -0.08367 | 0.00091 |
| 3 | 6 | 1.55603 | 6 | X | 0.00072 | -7.82068 | 0.00926 | -0.00018 |
| 4 | 8 | -0.04999 | | Y | -100.00125 | -10.39725 | -0.01199 | 0.00031 |
| 5 | 3 | 11.21631 | 7 | X | 100.00028 | -4.45972 | 0.00626 | -0.00007 |
| 6 | 5 | 4.24450 | | Y | -0.00382 | -3.71992 | -0.10274 | 0.00095 |
| 7 | 7 | -0.50891 | 8 | X | 0.00054 | -7.19476 | 0.00748 | -0.00013 |
| 8 | 4 | 8.16589 | | Y | 99.99866 | -3.08134 | -0.04344 | 0.00033 |

*Sequence of SCT control: 1,5→2,8→3,6→4,7

Table 8 is the results of the sequence control of an element, but then Table 9 shows the results of the simultaneous control of two elements. The two elements were selected according to the elongation e_{adj} of the CCS analysis results, and thus, the control sequence was determined. As shown in the table, the elements were controlled in the following order: 1, 5 → 2, 8 → 3, 6 → 4, 7. The errors that were produced in the control process were corrected, and the corrected adjustment $e_{adj}^{correct}$ slightly differed from that of the CCS analysis results. The maximum $e_{adj}^{correct}$ was 25.53423 cm, which was greater than that of the CCS results. This is similar to the result of the previous example, and is the result of the SCS control, unlike of the CCS control. Given the equilibrium analysis result, the ERR of the controlled displacement ranged from 0.0008% to 0.1027% compared with the target displacement, and the ERR0 considering the structure size also ranged from 0.00005% to 0.00095%, which makes the result reliable.

The both results of the CCS and the SCS considering the control sequence yielded a result close to the target shape and a better result by addressing errors through re-analysis by each stage. The errors produced in each SCS stage may be differed according to the elastic modulus of the structures and the size of the target displacement. As for the effective element, in the case of the IRCN model, elements 1, 2, 5 and 8 showed the greatest adjustment elongation, and this could also

be assessed visually.

4. Non-redundant element and maximum adjustment element

In the case of a RCN model and the IRCN model, effective control elements can be evaluated visually. However, this is difficult if there is a large number of elements or if the structure is complicated, and selection criteria are required. As explained about CCS and SCS virtual codes in Chapter 3, the independent elements or the maximum adjustment elongation could be the criteria. To explain the selection of the control elements in this manner, in this chapter, targeting the Geiger’s cable dome (GCD) model shown in Fig. 6, CCS control is conducted and the effective elements are observed. This model, similar to the IRCN model, is the same virtual model as the model designed to restore the initially designed shape from an imperfect shape, and was introduced by Kim *et al.* (2003). The GCD model, which has the element numbers and nodal numbers shown in Fig. (7), has 73 cables and 32 nodes, and the cable’s sectional area and nodal coordinates are shown in Table 10. The cable’s elastic modulus E is 160 GPa, and the cable is

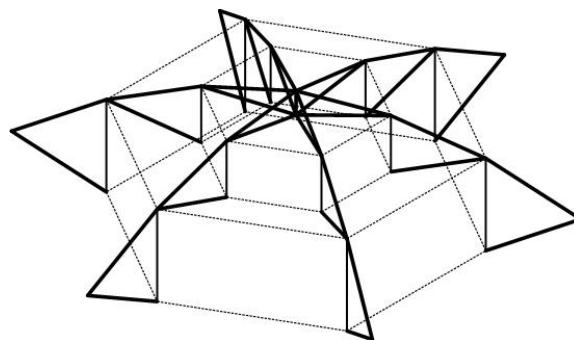


Fig. 6 Perspective view of the GCD model

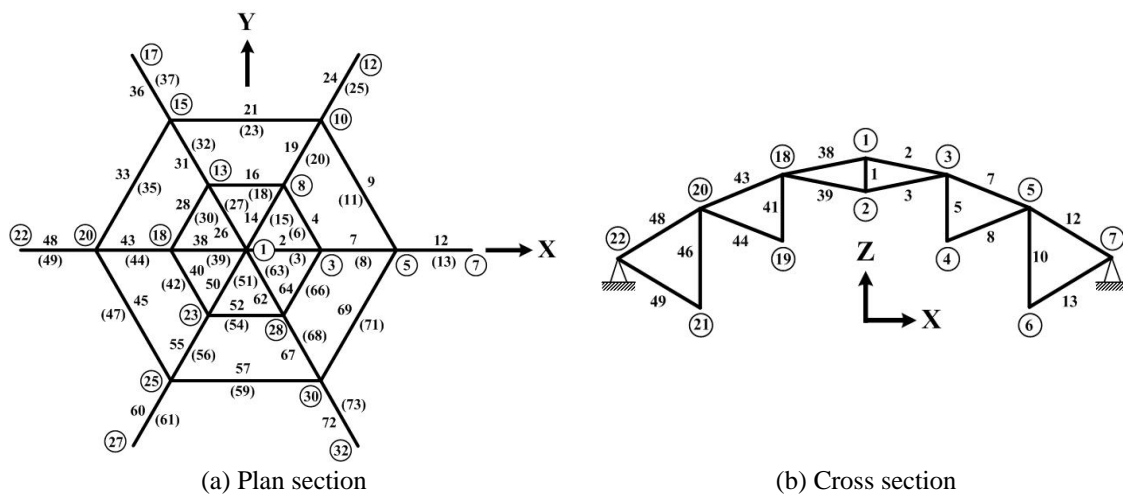


Fig. 7 Number of nodes and elements of the GCD model

Table 10 Cross-sectional area of cable and coordinate of the GCD model (unit: cm and cm², respectively)

| | | | | | | | |
|-------|------|------|------|------|------|-------|------|
| Elem. | 1 | 2 | 3 | 4 | 5 | 6 | 7 |
| Area | 1.00 | 0.01 | 0.01 | 0.01 | 1.00 | 0.02 | 0.02 |
| Elem. | 8 | 9 | 10 | 11 | 12 | 13 | |
| Area | 0.02 | 0.01 | 1.00 | 0.04 | 0.04 | 0.04 | |
| Node | 1 | 2 | 3 | 4 | 5 | 6 | 7 |
| X | 0.0 | 0.0 | 20.0 | 20.0 | 40.0 | 40.0 | 60.0 |
| Z | 21.0 | 15.0 | 18.5 | 4.5 | 11.5 | -11.5 | 0.0 |

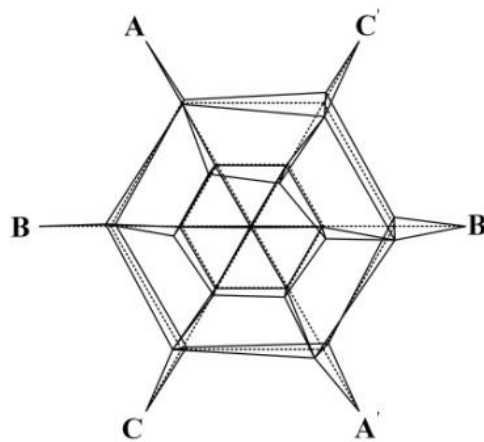


Fig. 8 Initial shape (solid line) and Target shape (dot line) of the GCD model

Table 11 Initial deformed coordinate of the GCD model (unit: cm)

| Node | X | Y | Z | Node | X | Y | Z | Node | X | Y | Z |
|------|---------|----------|----------|------|----------|----------|----------|------|----------|----------|----------|
| 1 | 1.13e-4 | -8.63e-5 | 2.09e+1 | 12 | 3.00e+1 | 5.19e+1 | 0.00e+0 | 23 | -9.99e+0 | -1.73e+1 | 1.84e+1 |
| 2 | 2.25e-4 | -1.16e-4 | 1.49e+1 | 13 | -9.99e+0 | 1.73e+1 | 1.84e+1 | 24 | -9.99e+0 | -1.73e+1 | 4.48e+0 |
| 3 | 2.00e+1 | -1.04e-4 | 1.84e+1 | 14 | -9.99e+0 | 1.73e+1 | 4.48e+0 | 25 | -1.99e+1 | -3.46e+1 | 1.14e+1 |
| 4 | 1.99e+1 | -4.05e-4 | 4.49e+0 | 15 | -1.99e+1 | 3.46e+1 | 1.14e+1 | 26 | -2.00e+1 | -3.46e+1 | -1.15e+1 |
| 5 | 3.99e+1 | 2.23e-4 | 1.14e+1 | 16 | -2.00e+1 | 3.46e+1 | -1.15e+1 | 27 | -3.00e+1 | -5.19e+1 | 0.00e+0 |
| 6 | 3.99e+1 | 7.56e-4 | -1.15e+1 | 17 | -3.00e+1 | 5.19e+1 | 0.00e+0 | 28 | 9.99e+0 | -1.73e+1 | 1.84e+1 |
| 7 | 6.00e+1 | 0.00e+0 | 0.00e+0 | 18 | -2.00e+1 | -9.27e-5 | 1.84e+1 | 29 | 9.99e+0 | -1.73e+1 | 4.49e+0 |
| 8 | 9.99e+0 | 1.73e+1 | 1.84e+1 | 19 | -1.99e+1 | -5.48e-5 | 4.48e+0 | 31 | 1.99e+1 | -3.46e+1 | 1.14e+1 |
| 9 | 9.99e+0 | 1.73e+1 | 4.49e+0 | 20 | -3.99e+1 | -5.52e-4 | 1.14e+1 | 31 | 1.99e+1 | -3.46e+1 | -1.15e+1 |
| 10 | 1.99e+1 | 3.46e+1 | 1.14e+1 | 21 | -4.00e+1 | 1.72e-4 | -1.15e+1 | 32 | 3.00e+1 | -5.19e+1 | 0.00e+0 |
| 11 | 1.99e+1 | 3.46e+1 | -1.15e+1 | 22 | -6.00e+1 | 0.00e+0 | 0.00e+0 | | | | |

classified into the upper cable, lower cable, ring cable and strut. The numbers in parentheses are the lower cable numbers. In the GCD model, the struts are all compression members, and this model is also known as the tensegrity dome. The boundary condition is that the outside nodes, that is, nodes 7, 12, 17, 22, 27 and 32, are fixed.

Similar to the IRCN model, the shapes, which were deformed due to the loosening of the cable tension, are shown in Fig. 8, and the corresponding nodal coordinates are shown in Table 11. In

Table 12 Target displacement of the GCD model (unit: cm)

| Node | 1 | 3 | 5 | 8 | 10 | 13 | 15 |
|------|---------|---------|---------|---------|---------|---------|---------|
| X | -0.0113 | 0.0000 | 0.4000 | 0.0400 | 0.1000 | -0.0600 | -0.2000 |
| Y | 0.0086 | 0.0104 | -0.0223 | 0.0510 | 0.3020 | 0.0510 | 0.3020 |
| Z | 1.2000 | 1.0000 | 1.1000 | 1.0000 | 1.2000 | 1.0000 | 1.1000 |
| Node | 18 | 20 | 23 | 25 | 28 | 30 | |
| X | 0.0000 | -0.3000 | -0.0700 | -0.2000 | 0.0300 | 0.1000 | |
| Y | 0.0093 | 0.0552 | -0.0510 | -0.3020 | -0.0510 | -0.3020 | |
| Z | 0.9000 | 1.2000 | 1.0000 | 1.1000 | 1.0000 | 1.2000 | |

Table 13 Result of the analysis of the GCD model using the CCS method (unit: cm)

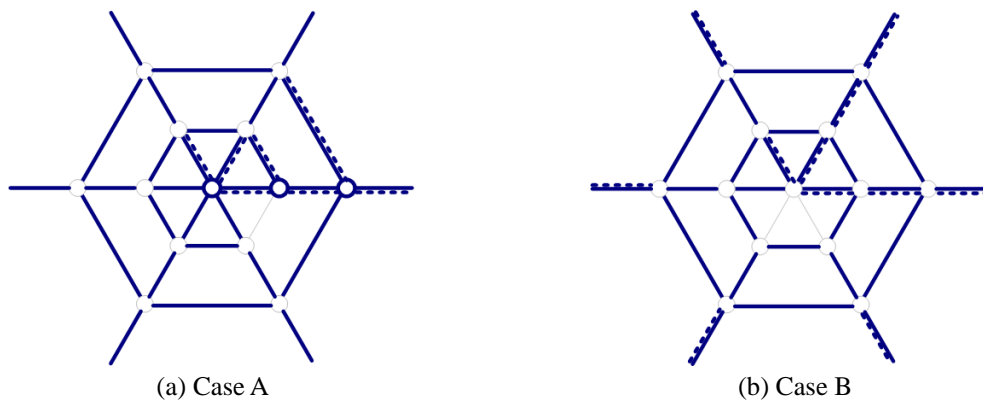
| Elem | order | e_{adj} | Elem | order | e_{adj} | Elem | order | e_{adj} | Elem | order | e_{adj} | Elem | order | e_{adj} |
|----------|-----------|---------------|-----------|-----------|--------------|-----------|-----------|--------------|-----------|----------|--------------|-----------|-----------|--------------|
| 1 | 72 | -0.071 | 16 | 50 | 0.999 | 31 | 23 | 2.382 | 46 | 48 | 1.316 | 61 | 14 | -2.799 |
| 2 | 63 | 0.361 | 17 | 60 | -0.399 | 32 | 30 | 1.930 | 47 | 22 | -2.440 | 62 | 52 | 0.966 |
| 3 | 66 | -0.305 | 18 | 38 | 1.777 | 33 | 16 | 2.637 | 48 | 5 | 3.375 | 63 | 69 | 0.242 |
| 4 | 71 | 0.151 | 19 | 42 | 1.674 | 34 | 46 | 1.404 | 49 | 15 | -2.776 | 64 | 62 | 0.381 |
| 5 | 67 | -0.280 | 20 | 33 | 1.834 | 35 | 21 | -2.454 | 50 | 49 | 1.052 | 65 | 59 | -0.503 |
| 6 | 40 | 1.733 | 21 | 9 | 3.000 | 36 | 24 | 2.343 | 51 | 61 | 0.386 | 66 | 39 | 1.735 |
| 7 | 4 | 3.445 | 22 | 44 | 1.517 | 37 | 13 | -2.847 | 52 | 51 | 0.999 | 67 | 41 | 1.721 |
| 8 | 36 | 1.790 | 23 | 19 | -2.499 | 38 | 68 | 0.260 | 53 | 56 | -0.846 | 68 | 32 | 1.839 |
| 9 | 1 | 4.308 | 24 | 6 | 3.275 | 39 | 58 | -0.582 | 54 | 37 | 1.780 | 69 | 2 | 3.922 |
| 10 | 43 | 1.545 | 25 | 11 | -2.937 | 40 | 70 | 0.171 | 55 | 26 | 2.335 | 70 | 45 | 1.457 |
| 11 | 17 | -2.531 | 26 | 55 | 0.854 | 41 | 53 | -0.965 | 56 | 29 | 1.935 | 71 | 18 | -2.517 |
| 12 | 27 | 2.010 | 27 | 64 | 0.358 | 42 | 34 | 1.825 | 57 | 8 | 3.000 | 72 | 7 | 3.275 |
| 13 | 10 | -2.960 | 28 | 73 | 0.060 | 43 | 31 | 1.840 | 58 | 47 | 1.344 | 73 | 12 | -2.889 |
| 14 | 54 | 0.867 | 29 | 57 | -0.742 | 44 | 28 | 1.980 | 59 | 20 | -2.472 | | | |
| 15 | 65 | 0.312 | 30 | 35 | 1.823 | 45 | 3 | 3.593 | 60 | 25 | 2.343 | | | |

the figure, the solid line is a deformed shape, and the dotted line is the target shape, as in the plan section in Fig. 7(a). Thus, the target displacement is the same as the difference between the two shapes. However, in roof structures as the GCD model, the upper surface nodes are an important control node mainly in shape control, because the shape of a structure is expressed by the outside curved surface. Thus, as shown in Table 17, the GCD model also sets the difference in the upper node coordinate value as the target displacement, uses the CCS method and analyzes the shape control.

The results of the control analysis of the GCD model are shown in Table 13, and the adjustment element was evaluated, targeting all the elements. The analysis results showed that the adjustment e_{adj} increased in the following order of the outside ring cables: 9, 69 and 45; and the internal ring cable 28 had the smallest control amount. Given the control results, the elements with a high adjustment were found to have been the outside ring cable and the outside upper cable, and the elements with a small control amount were found to have been the internal ring cable and the internal upper cable. The nodal displacement that was obtained from the control analysis was compared with the target displacement in Table 14. The error (ERR) against the target displacement ranged from 0.24% to 9.57%. The nodal error (ERRN) against the height of the

Table 14 Comparison of the target displacement with the adjusted displacement of the GCD model (unit: cm)

| Node | d_{tget} | d_{adj} | ERR (%) | ERRN (%) |
|------|------------|-----------|----------|----------|
| 1 | 1.2001 | 0.0176 | 1.462985 | 0.0008 |
| 3 | 1.0001 | 0.0918 | 9.180734 | 0.0044 |
| 5 | 1.1707 | 0.0102 | 0.871203 | 0.0005 |
| 8 | 1.0021 | 0.0700 | 6.986547 | 0.0033 |
| 10 | 1.2415 | 0.0095 | 0.766250 | 0.0005 |
| 13 | 1.0031 | 0.0960 | 9.565745 | 0.0046 |
| 15 | 1.1581 | 0.0086 | 0.739978 | 0.0004 |
| 18 | 0.9000 | 0.0732 | 8.128314 | 0.0035 |
| 20 | 1.2382 | 0.0105 | 0.851217 | 0.0005 |
| 23 | 1.0037 | 0.0184 | 1.836248 | 0.0009 |
| 25 | 1.1581 | 0.0066 | 0.568128 | 0.0003 |
| 28 | 1.0017 | 0.0876 | 8.745714 | 0.0042 |
| 30 | 1.2415 | 0.0031 | 0.246833 | 0.0001 |

Fig. 9 Non-redundant elements of the GCD model based on RREF(\mathbf{Y})

whole structure also ranged from 0.0001% to 0.0046%, which made the shape very close to the target shape.

In determining the control element, considering only the maximum control amount is not necessarily efficient control. To examine the effective cable and the influence of the control element in shape adjustment, the coefficient matrix \mathbf{Y} 's RREF in the control equations is calculated, thereby evaluating the non-redundant elements, that is, the linear independent elements. RREF(\mathbf{Y}) is determined differently according to the modeling of the structures, and despite a large number of cases, provides informations for the evaluation of the redundant elements and the non-redundant elements. The control of the non-redundant elements may directly impact the corresponding displacement, and the adjustment of the redundant elements may impact the interconnected displacements. Also, if the number of displacement components to be controlled and the number of linear independent elements are the same or small, the GCD model must have a solution for the control equations. This is because the controlled displacement component vector of the target model is not a null vector, and the number of controlled cables is greater than that of

the displacement components. Thus, the selection of the control element from the non-redundant elements is rational to control the displacement.

First, the RREF (Y) of the GCD model is evaluated considering two cases: one in which, as Fig. 7(b) shows, the cable elements are modeled into a radial form (Case A), and the other in which the element numbers are modeled from external elements into internal elements (Case B). The results of these cases are shown in Fig. 9. Here, the solid line represents the upper cable; the dotted line, the lower cable; and the circular, the struts.

As shown in the figures, in Case A, there were non-redundant elements in the upper cable and in the ring cable; and in Case B, the all outside upper cable elements are non-redundant elements. In Case A, the non-redundant elements also included the struts; and in Case B, they did not include the struts. Given the redundant elements in the two cases, the upper rings and the outside cables were mostly redundant. For results similar to these, modeling easily controllable elements first is helpful for configuring independent elements, and it is necessary to observe the redundant elements of a set of non-redundant elements through modeling associated with a numbering the cable elements.

Next, cable elements as same number of non-redundant elements were selected according to the element adjustment shown in Table 13, in descending order. The set of selected elements (Case C) is shown in Fig. 10. As shown in the figure, of the elements, the outside ring cables and the outside upper and lower cables were found to have had the greatest control amount. Compared with the results based on RREF(Y), there were both identical elements and non-identical elements.

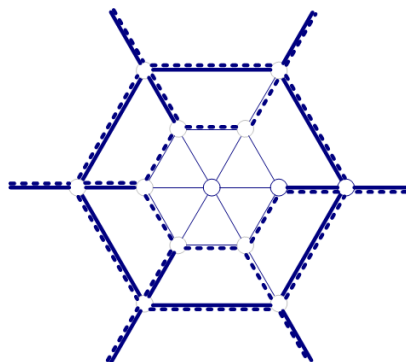


Fig. 10 Selected elements by e_{adj} in descending order (Case C)

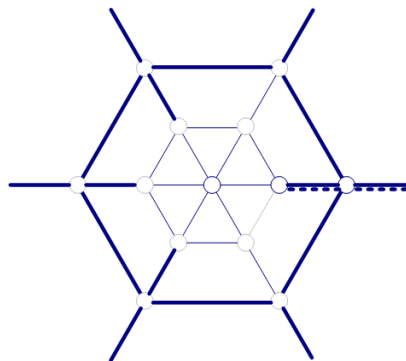


Fig. 11 Overlapped elements between the elements sets in cases A, B and C

Fig. 11 shows the intersection of the element sets in cases A, B and C. As shown in the figure, the outside upper cables and the outside upper ring cables were overlapped, and were found to have had the greatest effect. Considering the shape control of the structure's upper node and of the distorted shape in Fig. 8, the set of overlapped elements in Fig. 11 is noted as the efficient element for shape control.

5. Conclusions

Since cable structures are relatively light and are designed using the principle of the minimum surface, they can be suitable for planning spacious structures. However, it is difficult to construct the structures to create the shape intended by the designer, or to continue to maintain the initial shape. Readjustment of shapes that were deformed due to the loosening of the tension or the precise displacement control of the cables is drawing the attention of many researchers. This paper studied the shape control schemes of these pre-stressed cables and the effective control member. The process of deriving the control equations using the force method was explained, and the SCS and CCS were proposed as the control schemes. To explain the processes of such control schemes, a simple quadrilateral cable net model was set as a hypothetical model by classifying it into a regular model and an irregular model. The control analysis of the regular model, the concurrent and sequence control results proved reliable. Here, the sequence control produced errors in the control stage and differed according to the control sequence. In the control analysis of the irregular model, the concurrent control results proved relatively reliable, and the results of the analysis with the errors corrected in each stage were almost consistent with the target shape after the control. Finally, to investigate the control element, the Geiger cable dome model was adopted. By means of RREF analysis of the control equations' coefficient matrix, a set of non-redundant elements was evaluated. Also, using overlapping elements to the sets of selected elements, which were selected based on the control amount, important elements for shape control were assessed.

Acknowledgments

This research was supported by Basic Science Research Program through the National Research Foundation of Korea (NRF) funded by the Ministry of Education, Science and Technology (NRF-2014R1A2A1A01004473)

References

- Haftka, R.T. and Adelman, H.M. (1985a), "An analytical investigation of the static shape control of large space structures by applied temperatures", *AIAA J.*, **23**(3), 450-457.
- Haftka, R.T. and Adelman, H.M. (1985b), "Selection of actuator locations for static shape control of large space structures by heuristic integer programming", *Comput. Struct.*, **20**(1-3), 575-582.
- Irschik, H. (2002), "A review on static and dynamic shape control of structures by piezoelectric actuation", *Eng. Struct.*, **24**(1), 5-11.
- Burdisso, R.A. and Haftka, R.T. (1990), "Statistical analysis of static shape control in space structures", *AIAA J.*, **28**(8), 1504-1508.
- Furuya, H. and Haftka, R.T. (1995a), "Placing actuators on space structures by genetic algorithms and

- effectiveness indexes”, *Struct. Optim.*, **9**(2), 69-75.
- Furuya, H. and Haftka, R.T. (1995b), “Static shape control of space trusses with partial measurements”, *J. Spacecraft. Rocket.*, **32**(5), 856-865.
- Subramanian, G. and Mohan, P. (1996), “A fast algorithm for the static shape control of flexible structures”, *Comput. Struct.*, **59**(3), 485-488.
- Shea, K., Fest, E. and Smith, I.F.C. (2002), “Developing intelligent tensegrity structures with stochastic search”, *Adv. Eng. Inform.*, **16**(1), 21-40.
- Irschik, H., Heuer, R. and Ziegler, F. (1998), “Static shape control by applied strains without stress”, *Proceeding European Conference on Spacecraft Structures, Materials and Mechanical Testing*, Braunschweig, November.
- Irschik, H. and Ziegler, F. (2001), “Eigenstrain without stress and static shape control of structures”, *AIAA J.*, **39**(10), 1985-1990.
- Ziegler, F. (2005), “Computational aspects of structural shape control”, *Comput. Struct.*, **83**, 1191-1204.
- Nyashin, Y., Likhov, V. and Ziegler, F. (2005), “Stress-free displacement control of structures”, *Acta Mechanica*, **175**, 45-56.
- Tanaka, H. and Natori, M.C. (2006), “Shape control of cable net structures based on concept of self-equilibrated stresses”, *JSME Int. J. Ser. C: Mech. Syst., Mach. Elem. Manuf.*, **49**(4), 1067-1072.
- Tanaka, H., Shimozono, N. and Natori, M.C. (2008), “A design method for cable network structures considering the flexibility of supporting structures”, *Tran. Jpn. Soc. Aeronaut. Space Sci.*, **50**(170), 267-273.
- Tanaka, H. (2011), “Surface error estimation and correction of a space antenna based on antenna gain analyses”, *Acta Astronautica*, **68**(7-8), 1062-1069.
- You, Z. (1997), “Displacement control of pre-stressed structures”, *Comput. Meth. Appl. Mech. Eng.*, **144**(1-2), 51-59.
- Kwan, A.S.K. and Pellegrino, S. (1993), “Prestressing a space structures”, *AIAA J.*, **31**(10), 1961-1963.
- Kim, S.D., Jeong, E.S., Koo, H.S., Lee, H.H. and Jung, H.M. (2003), “Nonlinear constructional analysis of cable-dome structures for adjusting the initial stresses”, *IASS/APCS 2003 Symposium*, Taipei, October.
- Jeong, E.S., Kang, C.H., Lee, S.J., Park, S.W. and Kim, S.D. (2006), “Nonlinear constructional analysis of Zetlin-typed cable dome structures considering geometrical nonlinearity”, *IASS/APCS 2006 Symposium*, Beijing, October.
- Li, T. and Wang, Y. (2009), “Performance relationships between ground model and space prototype of deployable space antennas”, *Acta Astronautica*, **65**(9-10), 1383-1392.
- Li, T. and Ma, Y. (2011), “Robust vibration control of flexible cable-strut structure with mixed uncertainties”, *J. Vib. Control*, **17**(9), 1407-1416.
- Liu, M.Y., Lin, L.C. and Wang, P.H. (2012), “Investigation on deck-stay interaction of cable-stayed bridges with appropriate initial Shapes”, *Struct. Eng. Mech.*, **43**(5), 691-709
- Zribi, M., Almutairi, N.B. and Abdel, M.R. (2006), “Control of vibrations due to moving loads on suspension bridges”, *J. Eng. Mech.*, **132**(6), 659-670.
- Quelle, I.G. (2009), “Cable roofs. Evolution, classification and future trends, in: evolution and trends in design, analysis and construction of shell and spatial structures”, *IASS Symposium 2009*, Valencia, Spain.
- Pellegrino, S. (1993), “Structural computations with the SVD of the equilibrium matrix”, *Int. J. Solid. Struct.*, **30**(21), 3025-3035.
- Kwan, A.S.K. (1998), “A new approach to geometric nonlinearity of cable structures”, *Comput. Struct.*, **67**, 243-252.